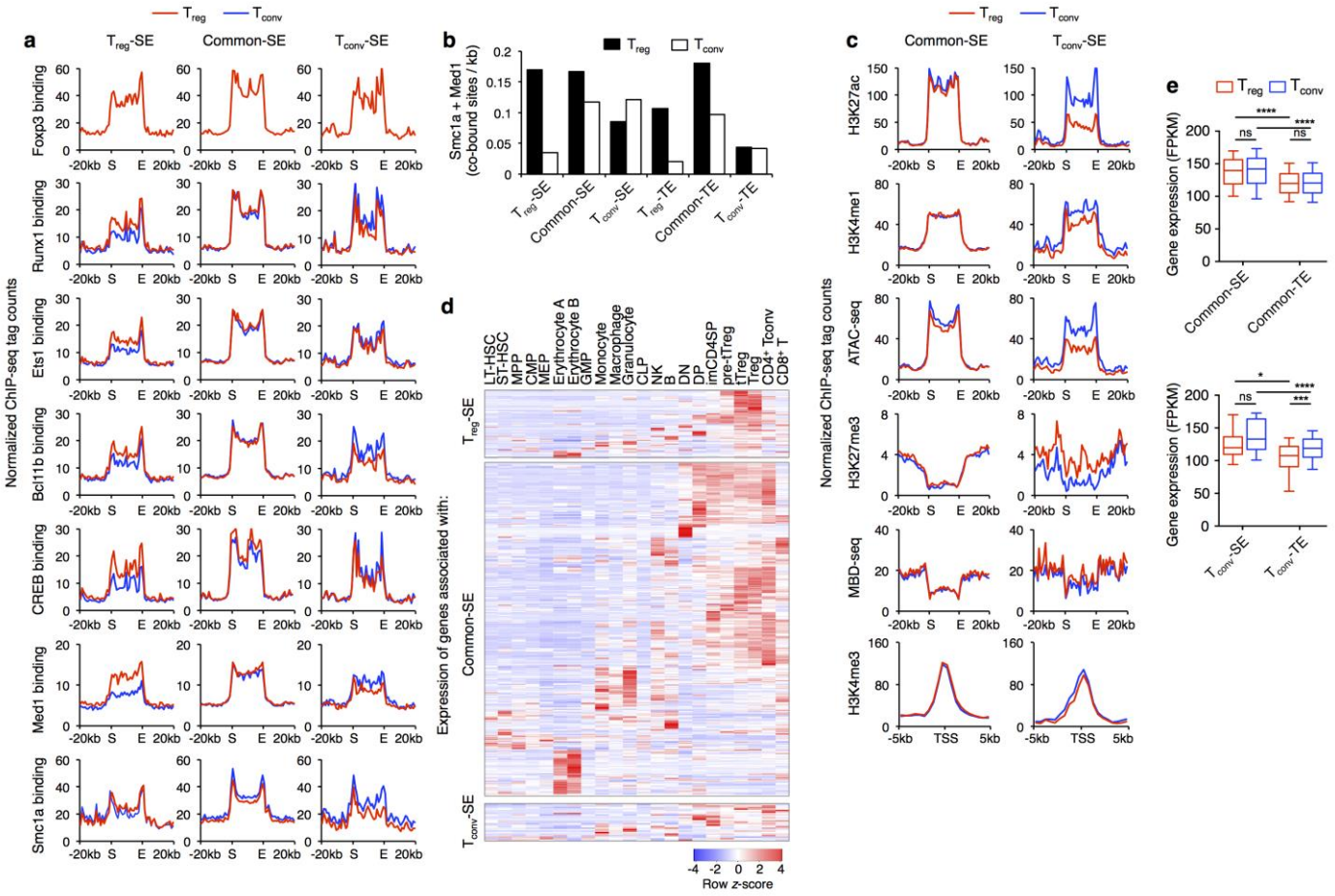


**Supplementary Figure 1**

Characteristics of SEs in $T_{reg}$ and $T_{conv}$ cells.

(**a**) Patterns of indicated transcription factor-binding at SEs and surrounding regions in $T_{reg}$ and $T_{conv}$ cells. Average normalized ChIP-seq signals of global $T_{reg}$-SEs, common-SEs or $T_{conv}$-SEs were plotted for merged SE regions ± 20 kb. Merged ends of SEs are marked as S (start) and E (end). (**b**) Frequency of sites co-occupied by Smc1a and Med1 within indicated regions in $T_{reg}$ and $T_{conv}$ cells. (**c**) H3K27ac, H3K4me1 and H3K27me3, ATAC-seq, and MBD-seq signals at global common-SE and $T_{conv}$-SE regions and H3K4me3 signal around transcription start sites (TSS) of common- or $T_{conv}$-SE-associated genes in $T_{reg}$ and $T_{conv}$ cells. Average normalized ChIP-seq density of common- or $T_{conv}$-SEs is plotted for merged SE regions ± 20 kb or TSS ± 5 kb. Merged ends of SEs are marked as S (start) and E (end). (**d**) Heatmap showing the expression of genes associated with $T_{reg}$-SE, common-SE or $T_{conv}$-SE in indicated immune cells. LT-HSC: long-term hematopoietic stem cell, ST-HSC: short-term hematopoietic stem cell, MPP: multipotent progenitor, CMP: common myeloid progenitor, MEP: megakaryocyte-erythrocyte progenitor, GMP: granulocyte-monocyte progenitor, and CLP: common lymphoid progenitor. (**e**) Expression of genes associated with common-SEs (334 genes) or -TEs (3516 genes) (left) and with $T_{conv}$-SEs (19 genes) or -TEs (146 genes) (right) in $T_{reg}$ and $T_{conv}$ cells. Average of two independent RNA-seq experiments are plotted in box-and-whisker plot (median and 10-90 percentiles are shown). ns $P > 0.05$, * $P \leq 0.1$, *** $P \leq 0.001$, and **** $P \leq 0.0001$ (Kruskal-Wallis test, followed by Dunn's multiple comparisons test). Data are from one experiment (transcription factor ChIP-seq, ATAC-seq, H3K4me1 and H3K27me3 ChIP-seq), representative of two independent experiments (H3K27ac ChIP-seq, H3K4me3 ChIP-seq and MBD-seq) (**a-c**), or are average of two independent experiments (RNA-seq) (**d,e**).

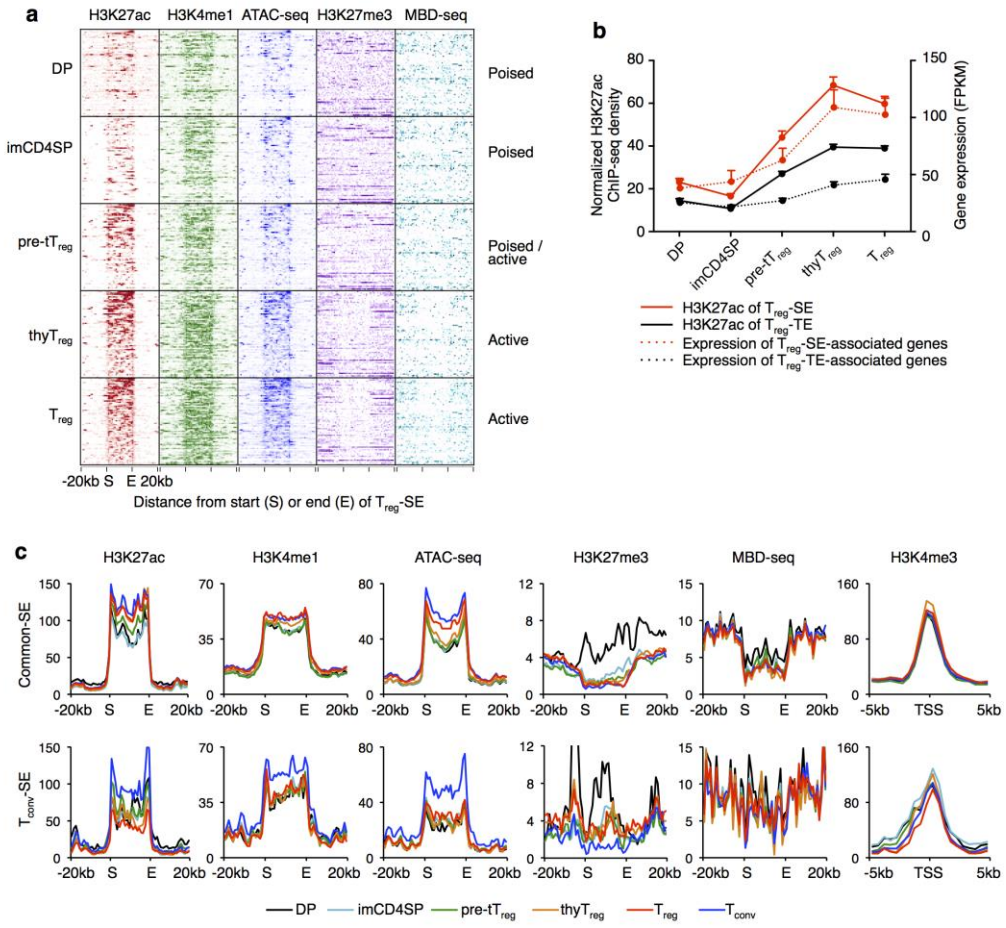


**Supplementary Figure 2**

Chromatin configuration changes at SE regions in developing $tT_{reg}$ cells.

(**a**) Heatmaps showing various epigenetic modifications at individual $T_{reg}$-SE regions in DP, immature CD4SP (imCD4SP), $tT_{reg}$ precursor (pre-$tT_{reg}$), thymic $T_{reg}$ (thy$T_{reg}$) and peripheral $T_{reg}$ cells. Individual $T_{reg}$-SEs (row) are listed in the same order in all sections and normalized ChIP-seq signals are shown for $T_{reg}$-SE regions with merged ends ± 20 kb. Overall status of $T_{reg}$-SEs suggested by combination of histone marks is indicated (right). (**b**) H3K27ac signals at $T_{reg}$-SE and $T_{reg}$-TE regions and associated gene expression during $T_{reg}$ cell development. Average of normalized ChIP-seq signals per kb at 66 $T_{reg}$-SEs or average FPKM of associated genes (± SEM) are plotted. (**c**) H3K27ac, H3K4me1 and H3K27me3, ATAC-seq, and MBD-seq signals at global common-SE and $T_{conv}$-SE regions and H3K4me3 signal around transcription start sites (TSS) of common- or $T_{conv}$-SE-associated genes in indicated cells. Average normalized ChIP-seq density of common- or $T_{conv}$-SEs is plotted for merged SE regions ± 20 kb or TSS ± 5 kb. Merged ends of SEs are marked as S (start) and E (end). Data in **a**–**c** are from one experiment (ATAC-seq, H3K4me1 and H3K27me3 ChIP-seq), representative of two independent experiments (H3K27ac ChIP-seq, H3K4me3 ChIP-seq and MBD-seq), or average of two independent experiments (RNA-seq).

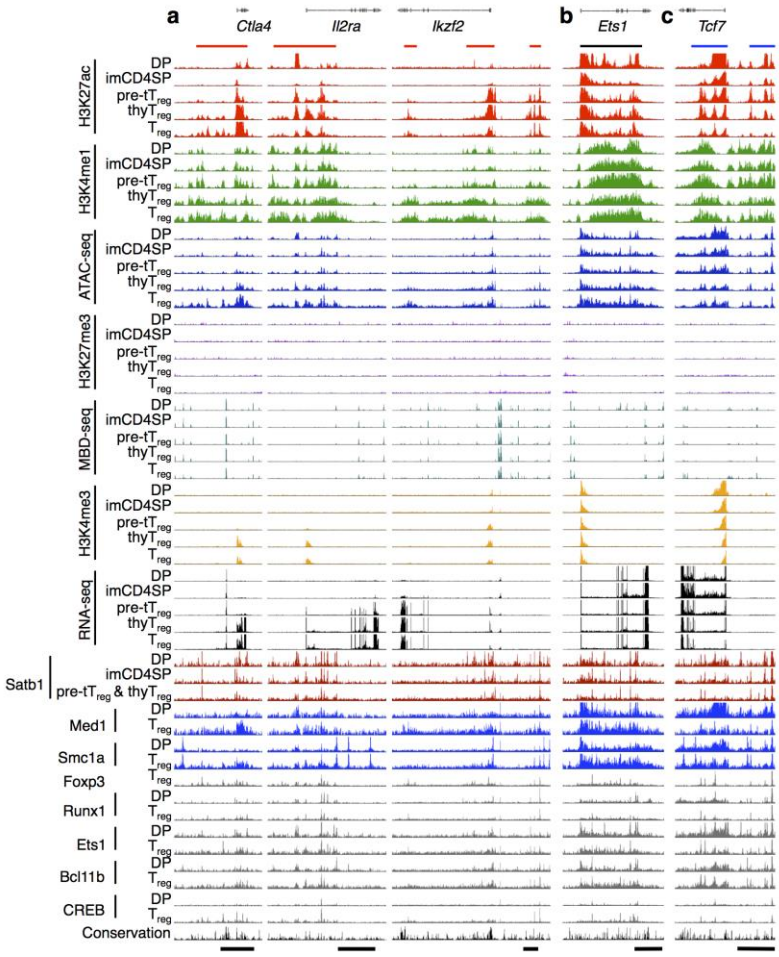


**Supplementary Figure 3**

Establishment of individual SEs in developing $tT_{reg}$ cells.

(**a-c**) Changes in various epigenetic modifications, mRNA transcription and transcription factor binding during $T_{reg}$ cell development around representative $T_{reg}$-SE regions at the *Ctla4*, *Il2ra* and *Ikzf2* loci (**a**), common-SE region at the *Ets1* locus (**b**) and $T_{conv}$-SE region at the *Tcf7* locus (**c**). H3K27ac, H3K4me1, H3K27me3, ATAC-seq, MBD-seq and RNA-seq signals in DP, immature CD4SP (imCD4SP), $tT_{reg}$ precursor (pre-$tT_{reg}$), thymic $T_{reg}$ (thy$T_{reg}$) and peripheral $T_{reg}$ cells, binding of various transcription factors in DP and $T_{reg}$ cells, and vertebrate conservation score are shown. Bars indicate 25 kb. Data are from one experiment (ATAC-seq, H3K4me1 and H3K27me3 ChIP-seq), representative of two independent experiments (H3K27ac ChIP-seq, H3K4me3 ChIP-seq and MBD-seq), or average of two independent experiments (RNA-seq).

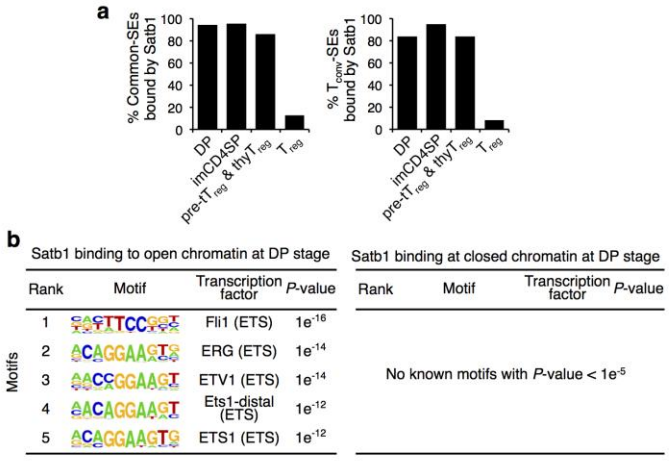


**Supplementary Figure 4**

Satb1 binding to SEs and transcription factor binding motifs of Satb1-binding sites at the DP stage.

(**a**) Percentage of common-SEs and $T_{conv}$-SEs occupied by Satb1 in indicated cell populations. (**b**) Enrichment of transcription factor-binding motifs in Satb1-binding sites at open chromatin (left) and at closed chromatin (right) within $T_{reg}$-SEs at the DP stage. Data are from one experiment (**a,b**).

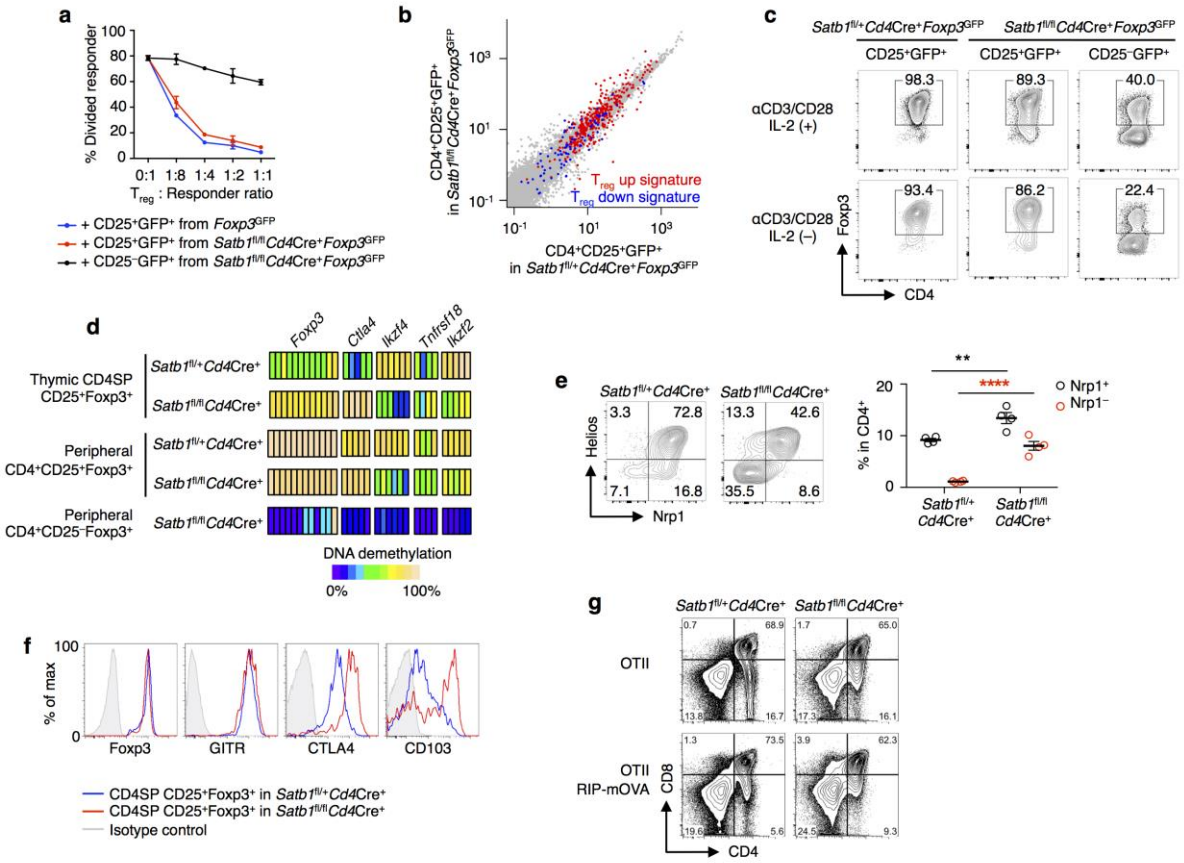


**Supplementary Figure 5**

Effects of T cell–specific *Satb1* deletion on characteristics of $T_{reg}$ cells and on thymic negative selection.

(**a**) Suppressive function of peripheral $CD4^+CD25^+GFP^+$ cells from *Satb1*$^{fl/+}$*Cd4*Cre$^+$*Foxp3*$^{GFP}$ and $CD4^+CD25^+GFP^+$ and $CD4^+CD25^-GFP^+$ cells from *Satb1*$^{fl/fl}$*Cd4*Cre$^+$*Foxp3*$^{GFP}$ mice. Percentages of divided naive $CD4^+$ T cells when cultured at indicated ratio with $T_{reg}$ cells are shown (mean ± SEM). (**b**) Scatter plot displaying global gene expression in $CD4^+CD25^+GFP^+$ cells from *Satb1*$^{fl/+}$*Cd4*Cre$^+$*Foxp3*$^{GFP}$ and *Satb1*$^{fl/fl}$*Cd4*Cre$^+$*Foxp3*$^{GFP}$ mice. Average normalized fragments per kilobase of transcript per million reads mapped (FPKM) values from two independent RNA-seq experiments are plotted and $T_{reg}$ up and down signature genes are highlighted. (**c**) Flow cytometry of indicated cells after *in vitro* culture with TCR stimulation, with or without IL-2, for the expression of Foxp3. Numbers indicate percentages of $Foxp3^+$ cells in live $CD4^+$ T cells. (**d**) DNA methylation status of the $T_{reg}$ cell signature genes in thymic and peripheral $CD4^+CD25^+Foxp3^+$ T cells from *Satb1*$^{fl/+}$*Cd4*Cre$^+$ and *Satb1*$^{fl/fl}$*Cd4*Cre$^+$ mice, and peripheral $CD4^+CD25^-Foxp3^+$ T cells from *Satb1*$^{fl/fl}$*Cd4*Cre$^+$ mice. (**e**) Flow cytometry of $CD25^+Foxp3^+$ $T_{reg}$ cells from 4-week-old *Satb1*$^{fl/+}$*Cd4*Cre$^+$ and *Satb1*$^{fl/fl}$*Cd4*Cre$^+$ mice for the expression of Nrp1 and Helios, and summary graph showing the percentages of $Nrp1^-CD25^+Foxp3^+$ and $Nrp1^+CD25^+Foxp3^+$ cells among $CD4^+$ T cells (mean ± SEM, n = 4). ** $P \le 0.01$ and **** $P \le 0.0001$ (two-way ANOVA, followed by Holm-Sidak's multiple comparison test). (**f**) Flow cytometry of $CD25^+Foxp3^+$ CD4SP cells found in the thymus of 4-week-old *Satb1*$^{fl/+}$*Cd4*Cre$^+$ and *Satb1*$^{fl/fl}$*Cd4*Cre$^+$ mice, for the expression of $T_{reg}$ cell signature and activation-associated molecules. (**g**) Flow cytometry of $Va2^+$ thymocytes from *Satb1*$^{fl/+}$*Cd4*Cre$^+$OTII, *Satb1*$^{fl/+}$*Cd4*Cre$^+$OTII-RIP-mOVA, *Satb1*$^{fl/fl}$*Cd4*Cre$^+$OTII, and *Satb1*$^{fl/fl}$*Cd4*Cre$^+$OTII-RIP-mOVA mice, for the examination of CD4SP thymocyte percentage. Data are representative or summary of three independent experiments with three or more mice (**a,c-f**), of two experiments with two mice (**b**), and of four experiments with four or more mice (**g**).

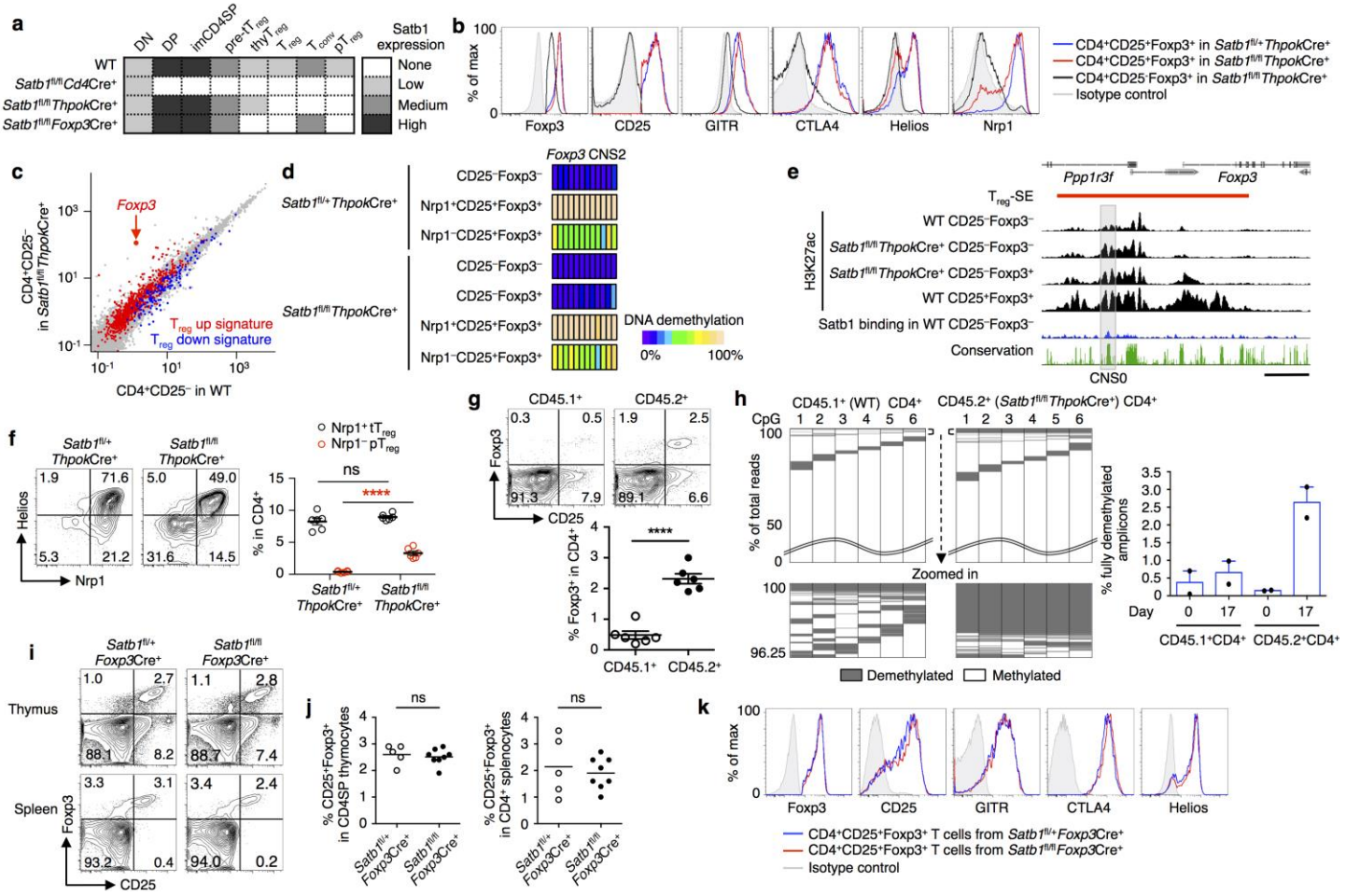


**Supplementary Figure 6**

Effects of mature CD4$^+$ T cell–specific and $T_{reg}$-specific *Satb1* deletion on $T_{reg}$ development, phenotype and $T_{reg}$-type DNA hypomethylation.

(**a**) Schematic diagram illustrating the timing of Satb1 deletion in *Satb1*$^{fl/fl}$*Cd4*Cre$^+$, *Satb1*$^{fl/fl}$*Thpok*Cre$^+$, and *Satb1*$^{fl/fl}$*Foxp3*Cre$^+$ mice. Satb1 expression level is indicated by color code. (**b**) Flow cytometry of peripheral CD4$^+$CD25$^+$Foxp3$^+$ T cells from *Satb1*$^{fl/+}$*Thpok*Cre$^+$ and *Satb1*$^{fl/fl}$*Thpok*Cre$^+$ mice, and CD4$^+$CD25$^-$Foxp3$^+$ T cells from *Satb1*$^{fl/fl}$*Thpok*Cre$^+$ mice, for the expression of $T_{reg}$ cell signature molecules. (**c**) Scatter plot displaying global gene expression in CD4$^+$CD25$^-$ cells from wild-type (WT) and *Satb1*$^{fl/fl}$*Thpok*Cre$^+$ mice. Average normalized fragments per kilobase of transcript per million reads mapped (FPKM) values from two independent RNA-seq experiments are plotted and $T_{reg}$ up and down signature genes are highlighted. (**d**) DNA methylation status of the *Foxp3* CNS2 region in peripheral CD4$^+$CD25$^-$Foxp3$^-$, CD4$^+$CD25$^+$Foxp3$^+$Nrp1$^+$ and CD4$^+$CD25$^+$Foxp3$^+$Nrp1$^-$ cells from *Satb1*$^{fl/+}$*Thpok*Cre$^+$ and *Satb1*$^{fl/fl}$*Thpok*Cre$^+$ mice, and CD4$^+$CD25$^-$Foxp3$^+$ from *Satb1*$^{fl/fl}$*Thpok*Cre$^+$ mice. Each block indicates CpG residues within amplicons. (**e**) H3K27ac modification in indicated cell types and Satb1 binding in WT $T_{conv}$ cells at the *Foxp3* locus. Vertebrate conservation score and CNS0 region are shown. Bar indicates 5 kb. (**f**) Flow cytometry of peripheral CD25$^+$Foxp3$^+$ T cells in *Satb1*$^{fl/+}$*Thpok*Cre$^+$ and *Satb1*$^{fl/fl}$*Thpok*Cre$^+$ mice, for the expression of Nrp1 and Helios, and summary data showing the percentages of Nrp1$^+$ $tT_{reg}$ and Nrp1$^-$ $pT_{reg}$ cells in peripheral CD4$^+$ T cells (mean ± SEM, n = 6). ns $P > 0.05$ and **** $P \le 0.0001$ (two-way ANOVA, followed by Holm-Sidak's multiple comparison test). (**g**) Flow cytometry of CD45.1$^+$ and CD45.2$^+$ CD4$^+$ T cells from *Rag2*$^{-/-}$ mice, which received CD4$^+$CD25$^-$ CD45RB$^{hi}$ T cells from WT (CD45.1$^+$) and *Satb1*$^{fl/fl}$*Thpok*Cre$^+$ (CD45.2$^+$) mice, for identification of $T_{reg}$ cells by CD25 and Foxp3 expression. Summary graph shows percentages of Foxp3$^+$ cells among CD45.1$^+$ or CD45.2$^+$ T cells (n = 6, mean ± SEM). **** $P \le$ 0.0001 (two-tailed t-test). (**h**) DNA methylation status of 6 CpG residues within the *Foxp3* CNS2 in WT and Satb1-deficient CD4$^+$ T cells isolated on day 17 in the experiment described in **g**. CpGs from 5' end are numbered as 1-6 (column) and amplicons are ordered from the most demethylated ones (row). Demethylated or methylated status is indicated by color code. 0-50% of fully methylated amplicons are omitted for presentation, as the wavy lines indicate (upper panel). Top 3.75% of total reads, when ordered from the most demethylated clones, are zoomed in (bottom). Summary data of two independent experiments, showing the percentage of fully demethylated amplicons, are also shown (right). (**i**) Flow cytometry of CD4SP thymocytes and CD4$^+$ splenocytes from 4-day-old *Satb1*$^{fl/+}$*Foxp3*Cre$^+$ and *Satb1*$^{fl/fl}$*Foxp3*Cre$^+$ mice, for identification of $T_{reg}$ cells by the expression of Foxp3 and CD25. (**j**) Percentages of

$CD25^+Foxp3^+$ $T_{reg}$ cells among CD4SP thymocytes and $CD4^+$ splenocytes in 4-day-old *Satb1*$^{fl/+}$*Foxp3*$Cre^+$ (n = 5) and *Satb1*$^{fl/fl}$*Foxp3*$Cre^+$ mice (n = 8). Horizontal line indicates mean. ns $P > 0.05$ (two-tailed t-test). (**k**) Flow cytometry of peripheral $CD4^+CD25^+Foxp3^+$ $T_{reg}$ cells from 4-week-old *Satb1*$^{fl/+}$*Foxp3*$Cre^+$ and *Satb1*$^{fl/fl}$*Foxp3*$Cre^+$ mice, for $T_{reg}$ cell signature molecule expression. Data are representative or summary of three independent experiments with three or more mice (**b,d,f,g,i-k**), average of two independent RNA-seq experiments (**c**), representative of two independent experiments (**e**), or representative and summary of two independent experiments (**h**).

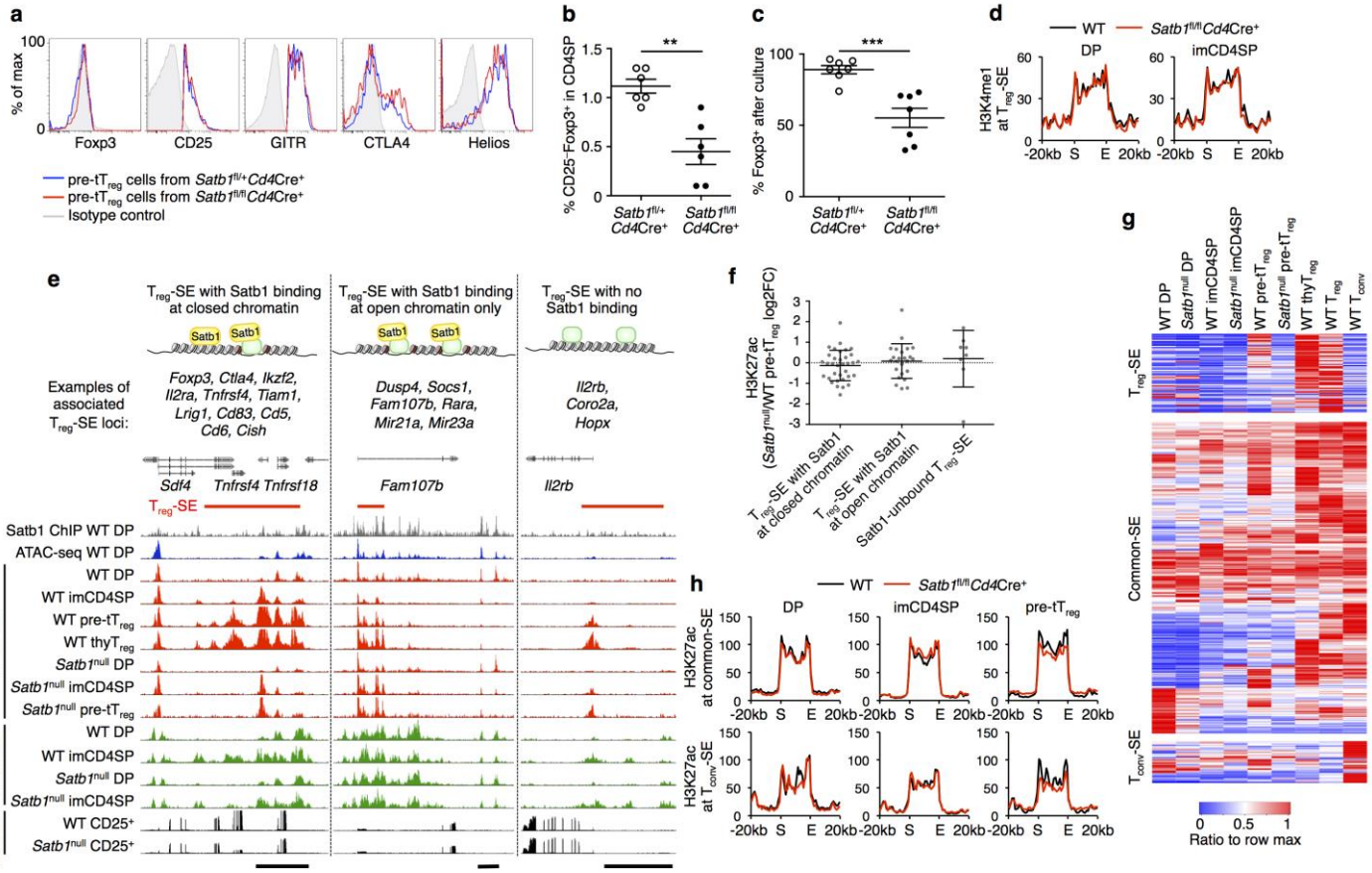


**Supplementary Figure 7**

Phenotypic and epigenetic characteristics of Satb1-deficient $tT_{reg}$ precursor cells.

(**a**) Flow cytometry of tTreg precursor (pre-$tT_{reg}$) cells from *Satb1*$^{fl/+}$*Cd4*Cre$^{+}$ and *Satb1*$^{fl/fl}$*Cd4*Cre$^{+}$ mice, for the expression of $T_{reg}$ cell signature molecules. (**b**) Percentages of CD25$^{-}$Foxp3$^{+}$ CD4SP thymocytes in 4-week-old *Satb1*$^{fl/+}$*Cd4*Cre$^{+}$ and *Satb1*$^{fl/fl}$*Cd4*Cre$^{+}$ mice. ** $P \leq 0.01$ (two-tailed t-test). (**c**) Percentages of Foxp3$^{+}$ cells after TCR and IL-2 stimulation of cells in **b**. *** $P \leq 0.001$ (two-tailed t-test). (**d**) H3K4me1 signals at global $T_{reg}$-SE regions in DP and immature CD4SP (imCD4SP) thymocytes from wild-type (WT) and *Satb1*$^{fl/fl}$*Cd4*Cre$^{+}$ mice. Average normalized ChIP-seq density of $T_{reg}$-SEs is plotted for merged $T_{reg}$-SE regions ± 20 kb. Merged ends of $T_{reg}$-SEs are marked as S (start) and E (end). (**e**) Categorization of $T_{reg}$-SEs by the chromatin state of initial Satb1 binding at the DP stage and effects of Satb1 deletion on their activation. $T_{reg}$-SEs are divided into those with at least one Satb1-binding site at closed chromatin (left), with Satb1-binding sites at open chromatin only (middle), or with no Satb1 binding at the DP stage. Schematic diagram illustrating the categorization by Satb1 binding type (top panel), examples of $T_{reg}$-SE loci (middle panel) and H3K27ac, H3K4me1 and gene transcription at representative $T_{reg}$-SE during $T_{reg}$ cell development in WT and *Satb1*$^{fl/fl}$*Cd4*Cre$^{+}$ mice (bottom) are shown for each category. Bars indicate 10 kb. (**f**) Summary data showing the effects of Satb1 deletion on $T_{reg}$-SEs categorized in **e**, shown as log2 fold-change (log2FC) of H3K27ac signal at $T_{reg}$-SEs between pre-$tT_{reg}$ cells of WT and *Satb1*$^{fl/fl}$*Cd4*Cre$^{+}$ mice (mean ± SEM). Dots indicate individual $T_{reg}$-SEs. (**g**) Heatmap showing relative H3K27ac signals at individual $T_{reg}$-SE, common-SE, and $T_{conv}$-SE regions in indicated cell populations. Ratio to the maximum value among the listed cell populations is shown. (**h**) H3K27ac signals at global common-SE and $T_{conv}$-SE regions in DP, imCD4SP and pre-$tT_{reg}$ cells from WT and *Satb1*$^{fl/fl}$*Cd4*Cre$^{+}$ mice. Average normalized ChIP-seq density of common-SEs or $T_{conv}$-SEs is plotted for merged SE regions ± 20 kb. Merged ends of SEs are marked as S (start) and E (end). Data are representative of three independent experiments with three or more mice (**a-c**), from one experiment (**d**), or representative of two independent experiments (**e-h**).

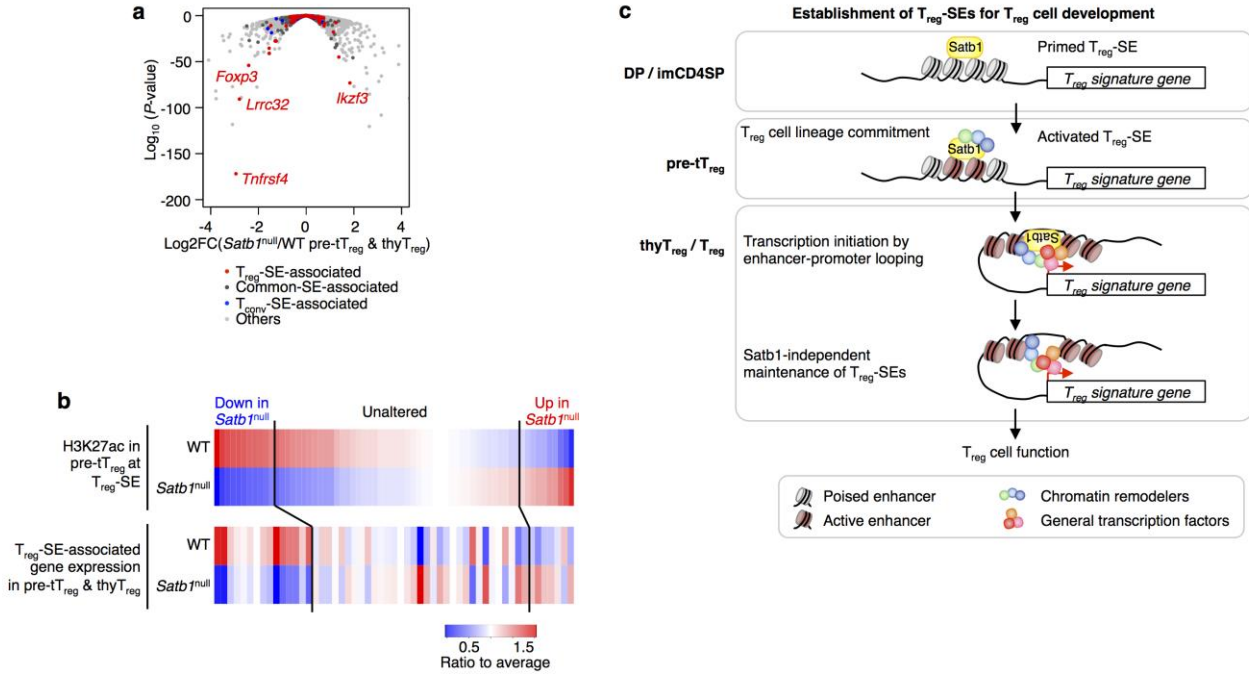


**Supplementary Figure 8**

Effects of Satb1-dependent $T_{reg}$-SE activation on associated gene expression.

(**a**) Volcano plot showing the differential gene expression between wild-type (WT) and *Satb1*$^{fl/fl}$*Cd4*Cre$^{+}$ CD24$^{+}$CD25$^{+}$GITR$^{+}$ CD4SP thymocytes (mixture of immature thymic $T_{reg}$ (thy$T_{reg}$) and t$T_{reg}$ precursor (pre-t$T_{reg}$) cells). Genes associated with $T_{reg}$-SEs, common-SEs and $T_{conv}$-SEs are highlighted. (**b**) H3K27ac of individual $T_{reg}$-SE regions at the pre-t$T_{reg}$ cell stage (top) and associated gene expression in CD24$^{+}$CD25$^{+}$GITR$^{+}$ CD4SP thymocytes (bottom) in WT and *Satb1*$^{fl/fl}$*Cd4*Cre$^{+}$ mice, shown as ratios to the average of two populations. $T_{reg}$-SEs are grouped into three categories by the effects of Satb1 deletion, as shown in Fig. 8e. (**c**) Hypothetical model of super-enhancer establishment and subsequent transcriptional regulation during thymic $T_{reg}$ cell development. $T_{reg}$-SE regions are poised at least from the DP stage and bound by Satb1. Upon receiving the signal to direct $T_{reg}$ cell differentiation, $T_{reg}$-SE regions undergo Satb1-dependent activation, likely through the recruitment of epigenetic modifying enzymes, and become $T_{reg}$ lineage-committed precursor cells. As $T_{reg}$ cell development proceeds, enhancer-promoter looping facilitates the expression of associated $T_{reg}$ cell signature genes, including *Foxp3*, as well as other epigenetic modifications such as $T_{reg}$-specific DNA demethylation, histone modification of promoter regions and chromatin loosening of enhancer and promoter regions. Once $T_{reg}$ cell development is complete, Foxp3 amplifies pre-established molecular features[1] and Satb1 transcription is repressed by Foxp3[2]; however, mediator, cohesin, and various transcription factors, including Foxp3, occupy the sites where Satb1 initially bound, maintaining the local chromatin structure.

1. Gavin, M.A. *et al.* Foxp3-dependent programme of regulatory T–cell differentiation. *Nature* **445**, 771–775 (2007).
2. Beyer, M. *et al.* Repression of the genome organizer SATB1 in regulatory T cells is required for suppressive function and inhibition of effector differentiation. *Nature immunology* **12**, 898–907 (2011).